

Supplemental Material for

A Computational Model Recapitulates Species-specific Differences in a Conserved Signaling Network

Adriana T. Dawes, David Wu, Karley K. Mahalak, Edward M. Zitnik, Natalia Kravtsova, Haiwei Su, and Helen M. Chamberlin

1 Supplemental Methods

Mathematical Model

Interaction network

To study nematode vulval development, we developed a biologically based mathematical model using data derived from experiments on *C. elegans*. We base our model on the interaction network in Fig 2, Main Text. Due to the conserved nature of the proteins involved, we have assumed that they are operating in a similar manner in *C. elegans* and *C. briggsae*. In contrast to previous models, we explicitly include input from the Wnt pathway in addition to the Ras/MAPK and Notch pathways.

Each arrow in the interaction network (Fig 2, Main Text) is supported by the following experimental evidence or expectations:

1. LIN-3 binds to LET-23, leading to LET-23 dimerization and cross-phosphorylation within LET-23 dimers. LIN-3, the *Caenorhabditis* epidermal growth factor (EGF), is released by the anchor cell and binds to the EGF receptor LET-23, which functions within the VPCs. LET-23 is the EGFR, and a receptor tyrosine kinase. Phosphorylated LET-23 is the active form. [1–6].
2. LET-23P activates LET-60. Active LET-23P stimulates formation of a complex including GRB2, GEF (both implicit to the model) and LET-60/Ras (a small GTPase). The GEF causes activation of the Ras GTPase LET-60 by facilitating exchange of GDP for GTP. [2, 5, 7, 8].
3. LET-60-GTP activates LIN-45. Activated LET-60-GTP leads to phosphorylation of LIN-45, a Raf protein, and initiates activation of the MAPK cascade [1, 9].
4. LIN-45P phosphorylates MEK-2. Phosphorylated LIN-45 then phosphorylates the MAP kinase kinase, MEK-2 [10, 11].
5. MEK-2P phosphorylates MPK-1. Phosphorylated MEK-2 then phosphorylates the MAP kinase, MPK-1 [10, 11].
6. MPK-1P phosphorylates LIN-1. Phosphorylated MPK-1 then phosphorylates LIN-1, an ETS domain protein. MPK-1P also phosphorylates LIN-31, a winged helix transcription factor, which forms a complex with LIN-1 (implicit to the model). Phosphorylation of each leads to disruption of the complex. [7, 10, 12–16].
7. MPK-1P activates SUR-2 Inactive. Active MPK-1 also activates SUR-2, a MED23 protein and part of the Transcriptional Mediator Complex. [17, 18].
8. LIN-1 suppresses synthesis of LIN-39. Phosphorylation of LIN-1 removes the inhibition of LIN-39 synthesis, allowing an increase of LIN-39 production [19, 20].

9. WNT enhances synthesis of LIN-39. Members of the WNT signaling pathway converge to promote synthesis of LIN-39 [21] or the activity of LIN-39 [22]. For simplicity, we assume a WNT ligand is secreted by the anchor cell, resulting in differential strength of the WNT signal, similar to the variable LIN-3 distribution across the VPCs. This model adapts to alternative hypotheses in which WNT signal arises from other sources (such as from multiple sources that would result in a uniform distribution of ligand) by altering the parameter that determines the steepness of the WNT gradient (parameter 69, WNTb).
10. LAG-2 and LIN-12 form a complex (L212). As the initial event in activation of the Notch signaling pathway, the Notch ligand LAG-2 binds to the receptor LIN-12 on the surface of the adjacent VPC [23].
11. L212 formation results in production of the NICD. L212, the complex formed by binding of LAG-2 and LIN-12, can either break apart into its component parts, or cause the irreversible cleavage of the intracellular domain of LIN-12 called NICD (Notch IntraCellular Domain) and release of the ligand LAG-2 [24].
12. NICD promotes synthesis of LIP-1. The cleaved intracellular domain of LIN-12, NICD, migrates to the nucleus where it promotes synthesis of the phosphatase LIP-1 [25].
13. NICD promotes synthesis of ARK-1. In addition, NICD promotes synthesis of the Ack-related tyrosine kinase ARK-1 [26].
14. LIN-1 inhibits synthesis of LAG-2. Synthesis of LAG-2, a transcriptional target of the EGF/Ras/MAPK pathway, is inhibited by the inactive, unphosphorylated form of LIN-1 [27]
15. SUR-2 Active promotes synthesis of LAG-2. Synthesis of LAG-2 is promoted by the active form of SUR-2 [27].
16. SUR-2 Active promotes decay of LIN-12. Active SUR-2 also promotes degradation of LIN-12 through an undefined mechanism [7, 17, 18, 28].
17. LIN-39 promotes synthesis of LAG-2 and LIN-12. LAG-2 and LIN-12 synthesis rely on the presence of LIN-39, even in the absence of the transcriptional regulator LIN-1 [20, 29]
18. LIP-1 promotes dephosphorylation of MPK-1P. The phosphatase activity of LIP-1 specifically targets MPK-1, resulting in dephosphorylation of MPK-1P. The activity of other phosphatases is implicit to the model, as they are not predicted to change in response to model inputs [25].
19. ARK-1 promotes decay of LET-23 through an unknown mechanism [26, 30, 31].

Model Assumptions

Before translating the interaction network into a system of equations, we make the following assumptions regarding the nature and form of the various interactions.

1. We implicitly incorporate the anchor cell by having a temporally constant EGF signal with spatially varying strength according to the position of the VPC.
2. We use coupled ordinary differential equations to construct the model.

3. We model interactions in the MAPK and Notch pathways using mass action or Michaelis-Menten kinetics.
4. We do not explicitly model the the activity of GEFs and GAPs on the interactions between LET-23 and LET-60.
5. We do not explicitly model the phosphorylation of LIN-39 by MPK-1.
6. We are representing the Wnt signaling pathway with a single model input, WNT. We assume this signal is temporally constant but can vary over space.
7. We are using LAG-2 as a proxy for members of the DSL family, and ARK-1 as a proxy for LST genes.

Each of these assumptions is made to simplify the model, for instance by grouping proteins according to functional modules, or assuming the cytoplasm is well mixed so that we can ignore intracellular concentration variability. Assumptions 1 and 6 derive from calculations of a steady state diffusion gradient from a point source with Dirichlet boundary conditions. We use a similar form for both the EGF and WNT signal in this model. Assumptions 2-3 specify the form of the model. We are assuming the cytoplasm is well mixed (Assumption 2), a similar assumption to other models [32, 33], and the assumption of Michaelis-Menten or Hill type kinetics (Assumption 3) reflects that interactions between proteins likely saturate at high concentrations, and we do not explicitly include intermediate complexes or interactions. Assumption 4 allows us to absorb the dynamics of these regulators into the relevant rate constants, while Assumption 5 is made since this phosphorylation event is not needed for LIN-39-mediated activity [19]. Assumption 7 allows us to group similar proteins into functional modules, for instance allowing LAG-2 to include the activity of APX-1 and DSL-1 [23].

Model Equations

Based on the interaction network and modeling assumptions discussed above, the vulval signaling network can be simulated using the following system of coupled ordinary differential equations. Variable names and definitions are given in Table 1 (Main text), and parameter names and median values are given in Tables S1 - S3.

$$\begin{aligned} \frac{dL23}{dt} &= k_{23}^+ - \left(k_{23_{min}}^- + (k_{23_{max}}^- - k_{23_{min}}^-) \frac{(AK1)^{n_{ak}}}{K_{ak}^{n_{ak}} + (AK1)^{n_{ak}}} \right) L23 \\ &\quad - k_{l3}^+ L23^2 \cdot LN3 + k_{l3}^- L23P \end{aligned} \quad (1a)$$

$$\frac{dL23P}{dt} = k_{l3}^+ L23^2 \cdot LN3 - k_{l3}^- L23P \quad (1b)$$

$$\frac{dL60}{dt} = -k_{60}^+ L60 \frac{(L23P)^{n_{23p}}}{K_{23p}^{n_{23p}} + (L23P)^{n_{23p}}} + k_{60}^- L60P \quad (1c)$$

$$\frac{dL60P}{dt} = k_{60}^+ L60 \frac{(L23P)^{n_{23p}}}{K_{23p}^{n_{23p}} + (L23P)^{n_{23p}}} - k_{60}^- L60P \quad (1d)$$

$$\frac{dL45}{dt} = -k_{45}^+ L45 \frac{L60P^{n_{60p}}}{K_{60p}^{n_{23p}} + L60P^{n_{60p}}} + k_{45}^- L45P \quad (1e)$$

$$\frac{dL45P}{dt} = k_{45}^+ L45 \frac{L60P^{n_{60p}}}{K_{60p}^{n_{23p}} + L60P^{n_{60p}}} - k_{45}^- L45P \quad (1f)$$

$$\frac{dMK2}{dt} = -k_{mk}^+ MK2 \frac{L45P^{n_{45p}}}{K_{45p}^{n_{45p}} + L45P^{n_{45p}}} + k_{mk}^- MK2P \quad (1g)$$

$$\frac{dMK2P}{dt} = k_{mk}^+ MK2 \frac{L45P^{n_{45p}}}{K_{45p}^{n_{45p}} + L45P^{n_{45p}}} - k_{mk}^- MK2P \quad (1h)$$

$$\begin{aligned} \frac{dMP1}{dt} &= -k_{mp}^+ MP1 \frac{MK2P^{n_{k2p}}}{K_{k2p}^{n_{k2p}} + MK2P^{n_{k2p}}} + k_{mpmin}^- MP1P \\ &\quad + k_{mpmax}^- MP1P \frac{LP1^{n_{lp1}}}{K_{lp1}^{n_{lp1}} + LP1^{n_{lp1}}} \end{aligned} \quad (1i)$$

$$\begin{aligned} \frac{dMP1P}{dt} &= k_{mp}^+ MP1 \frac{MK2P^{n_{k2p}}}{K_{k2p}^{n_{k2p}} + MK2P^{n_{k2p}}} - k_{mpmin}^- MP1P \\ &\quad - k_{mpmax}^- MP1P \frac{LP1^{n_{lp1}}}{K_{lp1}^{n_{lp1}} + LP1^{n_{lp1}}} \end{aligned} \quad (1j)$$

$$\begin{aligned} \frac{dLN1}{dt} &= -k_{l1}^+ LN1 \left(\frac{MP1P^{n_{p1p}}}{K_{p1p}^{n_{p1p}} + MP1P^{n_{p1p}}} \right) \\ &\quad + k_{l1}^- (1 - LN1) \end{aligned} \quad (1k)$$

$$\begin{aligned} \frac{dLN1P}{dt} &= -k_{l1}^+ LN1 \left(\frac{MP1P^{n_{p1p}}}{K_{p1p}^{n_{p1p}} + MP1P^{n_{p1p}}} \right) \\ &\quad - k_{l1}^- (1 - LN1) \end{aligned} \quad (1l)$$

$$\frac{dSR2I}{dt} = -k_{s2}^+ SR2I \frac{MP1P^{n_{p1p2}}}{K_{p1p2}^{n_{p1p2}} + MP1P^{n_{p1p2}}} + k_{s2}^- (1 - SR2I) \quad (1m)$$

$$\frac{dSR2A}{dt} = k_{s2}^+ SR2I \frac{MP1P^{n_{p1p2}}}{K_{p1p2}^{n_{p1p2}} + MP1P^{n_{p1p2}}} - k_{s2}^- (1 - SR2I) \quad (1n)$$

$$\frac{dL39}{dt} = k_{39}^+ WNT \left(1 - \frac{LN1^{n_{ln1}}}{K_{ln1}^{n_{ln1}} + (LN1)^{n_{ln1}}} \right) - k_{39}^- L39 \quad (1o)$$

$$\begin{aligned} \frac{dLG2}{dt} &= k_{lg2min}^+ \frac{L39^{n_{39}}}{K_{39}^{n_{39}} + L39^{n_{39}}} \\ &\quad \cdot \left(1 + k_{lg2max}^+ \left(1 - \frac{LN1^{n_{ln12}}}{K_{ln12}^{n_{ln12}} + LN1^{n_{ln12}}} \right) \left(\frac{(1 - SR2I)^{n_{sr2}}}{K_{sr2}^{n_{sr2}} + (1 - SR2I)^{n_{sr2}}} \right) \right) \\ &\quad - k_{lg2}^- LG2 - k_{2/12}^+ LG2 \cdot L12_{adj} + k_{2/12}^- L2/12 + k_{ni}^+ L2/12 \end{aligned} \quad (1p)$$

$$\begin{aligned} \frac{dL12}{dt} &= k_{n12}^+ \frac{L39^{n_{392}}}{K_{392}^{n_{392}} + L39^{n_{392}}} \\ &\quad - \left(k_{n12min}^- + (k_{n12max}^- - k_{n12min}^-) \frac{(1 - SR2I)^{n_{sr22}}}{(K_{sr22})^{n_{sr22}} + (1 - SR2I)^{n_{sr22}}} \right) L12 \\ &\quad - k_{2/12}^+ LG2_{adj} \cdot L12 + k_{2/12}^- L2/12_{adj} \end{aligned} \quad (1q)$$

$$\frac{dL2/12}{dt} = k_{2/12}^+ LG2 \cdot L12_{adj} - k_{2/12}^- L2/12 - k_{ni}^+ L2/12 \quad (1r)$$

$$\frac{dNIC}{dt} = k_{ni}^+ L2/12_{adj} - k_{ni}^- NIC \quad (1s)$$

$$\frac{dLP1}{dt} = k_{lp}^+ \left(\frac{(NIC)^{n_{nic}}}{K_{nic}^{n_{nic}} + (NIC)^{n_{nic}}} \right) - k_{lp}^- LP1 \quad (1t)$$

$$\frac{dAK1}{dt} = k_{ak}^+ \left(\frac{(NIC)^{n_{nic2}}}{K_{nic2}^{n_{nic2}} + (NIC)^{n_{nic2}}} \right) - k_{ak}^- AK1 \quad (1u)$$

We assume the following conservation laws:

$$L60P = L60_0 - L60 \quad (2a)$$

$$L45P = L45_0 - L45 \quad (2b)$$

$$MK2P = MK2_0 - MK2 \quad (2c)$$

$$MP1P = MP1P_0 - MP1 \quad (2d)$$

$$LN1P = LN1_0 - LN1 \quad (2e)$$

$$SR2A = SR2_0 - SR2I \quad (2f)$$

where the subscript 0 denotes the total concentration of that protein.

We also define the following characteristic concentrations for each variable:

$$LET - 23 : \quad \overline{L23} = \frac{k_{23}^+}{k_{23min}^-} \quad (3a)$$

$$LET - 23P : \quad \overline{L23P} = \frac{k_{l3}^+(k_{23}^+)^2}{k_{l3}^-(k_{23min}^-)^2} \quad (3b)$$

$$LET - 60 : \quad \overline{L60} = \overline{L60P} = L60_0 \quad (3c)$$

$$LIN - 45 : \quad \overline{L45} = \overline{L45P} = L45_0 \quad (3d)$$

$$MEK - 2 : \quad \overline{MK2} = \overline{MK2P} = MK2_0 \quad (3e)$$

$$MPK - 1 : \quad \overline{MP1} = \overline{MP1P} = MP1_0 \quad (3f)$$

$$LIN - 1 : \quad \overline{LN1} = \overline{LN1P} = LN1_0 \quad (3g)$$

$$SUR - 2 : \quad \overline{SR2I} = \overline{SR2A} = SR2I_0 \quad (3h)$$

$$LIN - 39 \quad \overline{L39} = \frac{k_{39}^+}{k_{39}^-} \quad (3i)$$

$$LAG - 2 : \quad \overline{LG2} = \frac{(1 + k_{lg2max}^+)k_{lg2min}^+}{k_{lg2}^-} \quad (3j)$$

$$LIN - 12 : \quad \overline{L12} = \frac{k_{lg2}^- k_{n12}^+ (k_{212}^- + k_{ni}^+)}{D} \quad (3k)$$

$$LAG - 2/LIN - 12 : \quad \overline{L2/12} = \frac{k_{n12}^+ k_{212}^+ k_{lg2min}^+ (1 + k_{lg2max}^+)}{D} \quad (3l)$$

$$NICD : \quad \overline{NIC} = \frac{k_{ni}^+ \overline{L212}}{k_{ni}^-} \quad (3m)$$

$$LIP - 1 : \quad \overline{LP1} = \frac{k_{lp}^+}{k_{lp}^-} \quad (3n)$$

$$ARK - 1 : \quad \overline{AK1} = \frac{k_{ak}^+}{k_{ak}^-} \quad (3o)$$

$$(3p)$$

After application of conservation laws and non-dimensionalization using the characteristic con-

centrations, we arrive at Eq 1 with the following following parameter groupings:

$$\kappa_{ak} = \frac{K_{ak}k_{ak}^-}{k_{ak}^+} \quad (4a)$$

$$\beta_{23} = \frac{k_{l3}^+k_{23}^+}{k_{23min}^-} \quad (4b)$$

$$\kappa_{23} = \frac{K_{23p}k_{l3}^-(k_{23min}^-)^2}{k_{l3}^+(k_{23}^+)^2} \quad (4c)$$

$$\kappa_{60p} = \frac{K_{60p}}{L600} \quad (4d)$$

$$\kappa_{45p} = \frac{K_{45p}}{L450} \quad (4e)$$

$$\kappa_{k2p} = \frac{K_{k2p}}{MK20} \quad (4f)$$

$$\kappa_{lp1} = \frac{K_{lp1}k_{lp}^-}{k_{lp}^+} \quad (4g)$$

$$\kappa_{p1p} = \frac{K_{p1p}}{MP10} \quad (4h)$$

$$\kappa_{p1p2} = \frac{K_{p1p2}}{MP10} \quad (4i)$$

$$\kappa_{ln1} = \frac{K_{ln1}}{LN10} \quad (4j)$$

$$\beta_{lg2} = \frac{k_{lg2}^-}{1 + k_{lg2max}^+} \quad (4k)$$

$$\kappa_{39} = \frac{K_{39}k_{39}^-}{k_{39}^+} \quad (4l)$$

$$\kappa_{ln12} = \frac{K_{ln12}}{LN10} \quad (4m)$$

$$\kappa_{sr2} = \frac{K_{sr2}}{SR2I0} \quad (4n)$$

$$\beta_{lg22} = \frac{k_{212}^+k_{lg2}^-k_{n12}^+(k_{212}^- + k_{ni}^+)}{k_{lg2}^-k_{212}^-k_{n12min}^- + k_{lg2}^-k_{ni}^+k_{n12min}^- + k_{212}^+k_{ni}^+k_{lg2min}^+ + k_{212}^+k_{ni}^+k_{lg2max}^+k_{lg2min}^+} \quad (4o)$$

$$\beta_{l12} = \frac{k_{lg2}^-k_{212}^-k_{n12min}^- + k_{lg2}^-k_{ni}^+k_{n12min}^- + k_{212}^+k_{ni}^+k_{lg2min}^+ + k_{212}^+k_{ni}^+k_{lg2max}^+k_{lg2min}^+}{k_{lg2}^-(k_{212}^- + k_{ni}^+)} \quad (4p)$$

$$\kappa_{392} = \frac{K_{392}k_{39}^-}{k_{39}^+} \quad (4q)$$

$$\kappa_{sr22} = \frac{K_{sr22}}{SR2I0} \quad (4r)$$

$$\beta_{l122} = \frac{k_{212}^+(1 + k_{lg2max}^+)k_{lg2min}^+}{k_{lg2}^-} \quad (4s)$$

$$\beta_{l123} = \frac{k_{212}^-k_{212}^+k_{lg2min}^+(1 + k_{lg2max}^+)}{k_{lg2}^-(k_{212}^- + k_{ni}^+)} \quad (4t)$$

$$\beta_{212} = k_{212}^- + k_{ni}^+ \quad (4u)$$

$$\kappa_{nic} = \frac{K_{nic}(k_{lg2}^- k_{212}^- k_{n12min}^- + k_{lg2}^- k_{ni}^+ k_{n12min}^- + k_{212}^+ k_{ni}^+ k_{lg2min}^+ + k_{212}^+ k_{ni}^+ k_{lg2max}^+ k_{lg2min}^+) k_{ni}^-}{k_{ni}^+ k_{n12}^+ k_{212}^+ k_{lg2min}^+ (1 + k_{lg2max}^+)} \quad (4v)$$

$$\kappa_{nic2} = \frac{K_{nic2}(k_{lg2}^- k_{212}^- k_{n12min}^- + k_{lg2}^- k_{ni}^+ k_{n12min}^- + k_{212}^+ k_{ni}^+ k_{lg2min}^+ + k_{212}^+ k_{ni}^+ k_{lg2max}^+ k_{lg2min}^+) k_{ni}^-}{k_{ni}^+ k_{n12}^+ k_{212}^+ k_{lg2min}^+ (1 + k_{lg2max}^+)} \quad (4w)$$

1.1 Model parameters

Parameter sampling and selection methods

To generate model parameter sets, we used two approaches: random selection, and a custom algorithm based on a Metropolis-Hastings random walk, see [34] for more details. The random selection method selects parameters using a uniform distribution across a specified range. The number of successful parameter sets generated using this method is small, and we use these parameter sets only to verify that parameter sets generated by the custom random walk method have the same general characteristics (Fig S1). Note that since the model is non-dimensionalized and parameter groupings are being varied, it is possible for ratios of parameters to vary over many orders of magnitude, even though the original biochemical parameters may be more constrained. The custom random walk algorithm randomly generates parameter sets until one is found that produces a wild-type pattern at steady state. This successful parameter set is then used as a basis to generate the next parameter set. If the new parameter set fails to produce a wild-type pattern at steady state, the most recent successful parameter set is used to generate the next parameter set. If the new parameter set does produce the wild-type pattern at steady state, the new parameter set is then used to generate the next parameter set. This is a significantly more efficient method for searching parameter space, and results in significant time savings when dealing with such a complex, high dimensional, nonlinear model. Parameter sets generated by the custom random walk algorithm are used for all of the analysis and results in this paper.

Parameter sets are declared to satisfy the wild-type pattern at steady state if the values for LAG-2 and LIP-1 fall within the ranges indicated in Fig 4, Main Text. Only a parameter set that satisfies all of these conditions for all six cells is considered a successful parameter set. These stringent requirements mean that we will reject parameter sets that take on intermediate LAG-2 or LIP-1 values, but the successful parameter sets will have well defined primary, secondary and tertiary states.

We then subject the successful parameter sets, those that produce the wild-type cell fate pattern at steady state, to an *in silico* treatment representing the activity of the drug U0126. Since U0126 interferes with the ability of MEK-2 to phosphorylate MPK-1, we reduce the value of the parameter k_{mp}^+ in increments of 10%, run the model to steady state and check the resulting pattern of cell fates. We ease the requirements for cell fates with the simulated drug treatment, and consider cells to be induced (either 1° or 2°), with LAG-2 or LIP-1 levels greater than 1/2, or not induced, with LAG-2 and LIP-1 levels less than 1/2, as summarized in Fig 4, Main Text. Parameter sets that have 0 or 1 induced cells at steady state with 30% of k_{mp}^+ are classified as *C. elegans*-like parameter sets while parameter sets that have 2 or 3 induced cells at steady state as classified as *C. briggsae*-like. Parameter sets that do not converge to a steady state solution at any level of k_{mp}^+ reduction are rejected. The final collection of parameter sets that we analyze in this paper contains those that produce the wild-type cell fate pattern when set to their default levels, converge to steady state at all levels of k_{mp}^+ reduction, and produce a *C. elegans* or *C. briggsae*-like level of

Table S1: Synthesis and decay parameters associated with Equations 1 - 15 (Main text).

Param Number	Param Name	Param Meaning	Median value (<i>C. elegans</i> / <i>C. briggsae</i>)
1	k_{23min}^-	Min LET-23 synthesis rate	0.0000050/0.0112
2	k_{23max}^-	Max LET-23 synthesis rate	0.000180/3.860581
3	k_{l3}^-	Phosphorylated LET-23 combined synthesis/decay rate	1.3613770/0.02729
4	k_{60}^+	LET-60 activation rate	0.39881/0.567288
5	k_{60}^-	LET-60 inactivation rate	0.188494/0.466115
6	k_{45}^+	LIN-45 phosphorylation rate	54.321606/1.015951
7	k_{45}^-	LIN-45 dephosphorylation rate	2.960295/5.225416
8	k_{mk}^+	MEK-2 phosphorylation rate	2.620564/0.109308
9	k_{mk}^-	MEK-2 dephosphorylation rate	0.002871/0.016059
10	k_{mp}^+	MPK-1 phosphorylation rate	0.00081/0.007338
11	k_{mpmin}^-	Min MPK-1 dephosphorylation rate	0.356764/2.540023
12	k_{mpmax}^-	Max MPK-1 dephosphorylation rate	8.91717/0.224846
13	k_{l1}^+	LIN-1 phosphorylation rate	9.362762/49.038736
14	k_{l1}^-	LIN-1 dephosphorylation rate	0.000467/3.221771
15	k_{s2}^+	SUR-2 activation rate	0.000143/0.546721
16	k_{s2}^-	SUR-2 deactivation rate	0.012386/0.017671
17	k_{39}^-	LIN-39 combined synthesis/decay rate	0.292151/0.219251
18	k_{lg2max}^+	Max LIN-1/SUR-2-mediated LAG-2 synthesis rate	5.470613/0.018851
19	k_{lg2}^-	LAG-2 decay rate	0.088846/0.288601
20	k_{n12min}^-	Min SUR-2-mediated LIN-12 decay	0.446686/0.47998
21	k_{n12max}^-	Max SUR-2-mediated LIN-12 decay	18.958819/17.29522
22	k_{ni}^-	NICD combined synthesis/decay rate	0.077458/0.116162
23	k_{lp}^-	LIP-1 combined synthesis/decay rate	3.297863/0.600168
24	k_{ak}^-	ARK-1 combined synthesis/decay rate	0.020583/0.084367
25	β_{23}	LET-23 combined phosphorylation/dephosphorylation rate	0.000209/0.011531
26	β_{lg2}	LIN-39-mediated LAG-2 synthesis rate	0.15496/0.486915
27	β_{lg22}	LAG-2/LIN-12 complex combined formation/dissociation rate	12.6360779/1.353046
28	β_{112}	LIN-12 synthesis rate	0.008836/0.067787
29	β_{1122}	LAG-2/LIN-12 complex formation rate	0.00634/0.002721
30	β_{1123}	LAG-2/LIN-12 complex dissociation rate	0.080158/0.039579
31	β_{212}	LAG-2/LIN-12 complex combined formation/dissociation rate	125.591339/19.52538

cell induction at 30% k_{mp}^+ . To determine the difference in timing between primary and secondary cell fate specification (Figure 1D), we subtracted the time at which the level of LIP-1 in P5.p/P7.p reached 2/3 from the time at which the level of LAG-2 in P6.p reached 2/3. While the model may not have reached steady state by these times, we assume that reaching the minimum threshold for primary or secondary cell fate specification is sufficient to indicate eventual cell fate.

Table S2: **Hill function half maximum parameters associated with Equations 1 - 15 (Main text).**

Param Number	Param Name	Param Meaning	Median value (<i>C. elegans</i> / <i>C. briggsae</i>)
32	κ_{ak}	ARK-1-mediated LET-23 synthesis half max value	0.012719/0.171808
33	κ_{23p}	LET-23P-mediated LET-60 activation half max value	0.013097/0.038117
34	κ_{60p}	LET-60-mediated LIN-45 phosphorylation half max value	0.022286/0.030986
35	κ_{45p}	LIN-45-mediated MEK-2 phosphorylation half max value	5.615752/0.505122
36	κ_{k2p}	MEK-2-mediated MPK-1 phosphorylation half max value	0.000803/0.012548
37	κ_{lp1}	LIP-1-mediated MPK-1 dephosphorylation half max value	28.387616/0.007598
38	κ_{p1p}	MPK-1-mediated LIN-1 phosphorylation half max value	0.001937/0.001971
39	κ_{p1p2}	MPK-1-mediated SUR-2 activation half max value	0.000852/0.028667
40	κ_{ln1}	LIN-1-mediated LIN-39 synthesis half max value	0.000630/3.490378
41	κ_{39}	LIN-39-mediated LAG-2 synthesis half max value	0.986741/0.861334
42	κ_{ln12}	LIN-1-mediated LAG-2 synthesis half max value	0.114556/0.104751
43	κ_{sr2}	SUR-2-mediated LAG-2 synthesis half max value	0.047615/0.135605
44	κ_{392}	LIN-39-mediated LIN-12 synthesis half max value	0.019304/0.004492
45	κ_{sr22}	SUR-2-mediated LIN-12 synthesis half max value	0.031232/0.040824
46	κ_{nic}	NICD-mediated LIP-1 synthesis half max value	0.003138/0.052019
47	κ_{nic2}	NICD-mediated ARK-1 synthesis half max value	0.079264/0.166385

Test of a model based on median parameter values for sensitivity to single parameter variation.

For one test of the sensitivity of our model to variation in parameter values we used one-factor-at-a-time analysis [35]. Results are summarized in Fig 10, Main Text. We determined the median value of each parameter from our final collection of successful *C. elegans* and *C. briggsae*-like parameter subsets, and using the parameter set containing the median value, we varied the parameter of interest from 0 to 200%, incrementing in steps of 10%. At each level of variation, we tested the models' response to simulated U0126 treatment and classified the response as *C. elegans*-like, *C. briggsae*-like or neither, according to the conditions detailed above. By considering the *C. elegans* and *C. briggsae*-like cases separately, we are able to determine which parameter values contribute to each phenotype.

Table S3: Hill function exponents and model inputs associated with Equations 1 - 15 (Main text).

Param Number	Param Name	Param Meaning	Median value (<i>C. elegans</i> / <i>C. briggsae</i>)
48	<i>nak</i>	ARK-1-mediated LET-23 synthesis Hill exponent	3/3
49	<i>n23p</i>	LET-23P-mediated LET-60 activation Hill exponent	3/3
50	<i>n60p</i>	LET-60-mediated LIN-45 phosphorylation Hill exponent	2/2
51	<i>n45p</i>	LIN-45-mediated MEK-2 phosphorylation Hill exponent	2/2
52	<i>nk2p</i>	MEK-2-mediated MPK-1 phosphorylation Hill exponent	2/3
53	<i>nlp1</i>	LIP-1-mediated MPK-1 dephosphorylation Hill exponent	3/3
54	<i>np1p</i>	MPK-1-mediated LIN-1 phosphorylation Hill exponent	3/2
55	<i>np1p2</i>	MPK-1-mediated SUR-2 activation Hill exponent	3/3
56	<i>nlm1</i>	LIN-1-mediated LIN-39 synthesis Hill exponent	2/2
57	<i>n39</i>	LIN-39-mediated LAG-2 synthesis Hill exponent	3/3
58	<i>nlm12</i>	LIN-1-mediated LAG-2 synthesis Hill exponent	2/2
59	<i>nsr2</i>	SUR-2-mediated LAG-2 synthesis Hill exponent	2/3
60	<i>n392</i>	LIN-39-mediated LIN-12 synthesis Hill exponent	3/2
61	<i>nsr22</i>	SUR-2-mediated LIN-12 synthesis Hill exponent	2/3
62	<i>nnic</i>	NICD-mediated LIP-1 synthesis Hill exponent	3/3
63	<i>nnic2</i>	NICD-mediated ARK-1 synthesis Hill exponent	3/2
64	<i>LN3a</i>	Max scaled value of spatially varying LIN-3 signal and signal strength at P6.p	1/1
65	<i>LN3b</i>	Steepness of LIN-3 gradient and LIN-3 signal strength at P5.p, P7.p	0.512052/0.487135
66	<i>LN3c</i>	LIN-3 signal strength at P4.p, P8.p, $LN3b^2$	0.262198/0.237301
67	<i>LN3d</i>	LIN-3 signal strength at P3.p, $LN3b^3$	0.134259/0.115598
68	<i>WNTa</i>	Max scaled value of spatially varying WNT signal and signal strength at P6.p	1/1
69	<i>WNTb</i>	Steepness of WNT gradient and WNT signal strength at P5.p, P7.p	0.18896/0.138278
70	<i>WNTc</i>	WNT signal strength at P4.p, P8.p, $WNTb^2$	0.035706/0.019121
71	<i>WNTd</i>	WNT signal strength at P3.p, $WNTb^3$	0.006747/0.002644

Test of all parameter sets to pathway blocking

The model was tested in response to a complete knockdown of a particular parameter. This was accomplished for each parameter set by setting the specified parameter to zero, then running the model to steady state. Value of LAG-2 and LIP-1 were assessed in each VPC and assigned the appropriate fate according Fig 4, Main Text. Results of this test are shown in Fig S3.

Test of phenotype switching

The model was tested to determining whether variation of a single parameter can cause the model with a *C. briggsae*-like parameter set to respond to simulated U0126 treatment with a *C. elegans*-like response, and vice versa. For each parameter set, first the target parameter was varied from 0 to 200% of its original value, then the parameter k_{mp}^+ , corresponding to U0126's point of action, was reduced to 30% of its original value. With these two parameter modifications, the model was run to steady state and the induction state of each VPC was determined according to Fig 4, Main Text. Results of this test are shown in Fig S4.

2 Supplemental Results

Model parameters that produce wild-type cell fate patterns are robust to variation.

Since our model can simulate wild-type developmental patterns, we wished to determine whether any parameters must be constrained in order to produce this output. We are not able to *a priori* specify parameter values in our model since it was built on observations of *in vivo* experimental manipulations, primarily genetic mutant analysis. This approach favors validation of the defined relationships, but means that model parameters are not known, and cannot currently be experimentally determined.

Consequently, we selected functional parameters for the model by sampling parameter space for sets that produce a wild-type pattern of cell fates using two different approaches as detailed above, Section 1.1. Of the 6735 parameter sets identified by the random walk method, we used 6490 parameter sets for the analysis presented in this paper, due to additional data considerations described below. We next asked whether any of the parameters are constrained and can only take on a limited range of values in order to produce the wild-type pattern, and found that the parameters can take on a wide range of values (Fig S1). This suggests there are no critically constrained parameters in the model and that our model is robust to parameter variation.

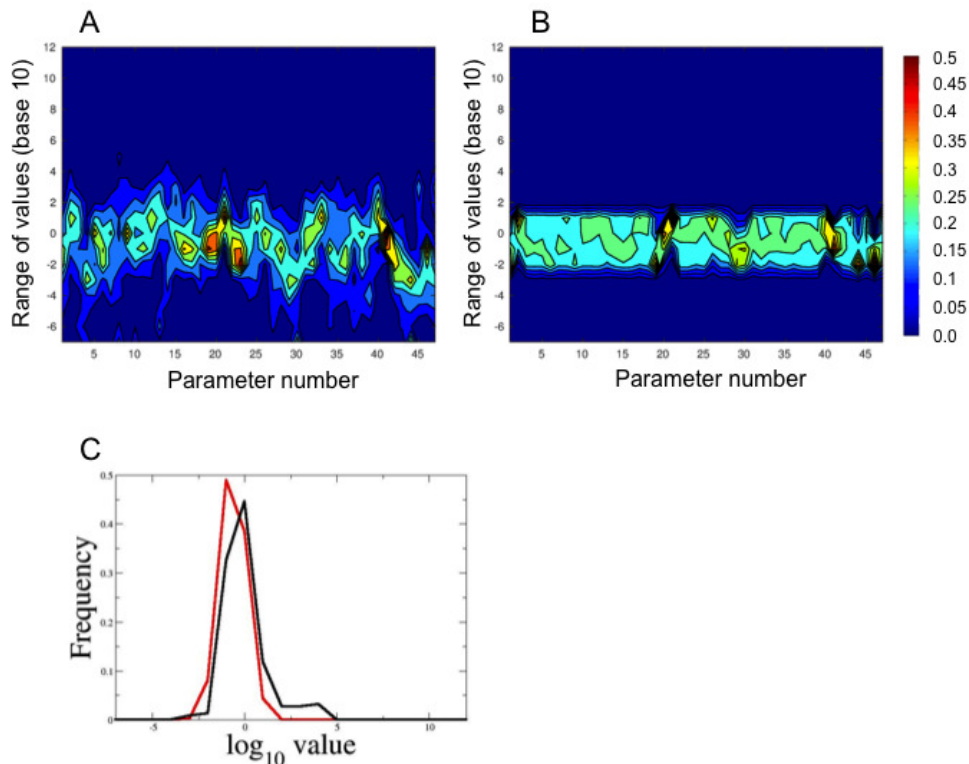


Figure S1: Wild-type model parameter values are robust to variation. (A, B) Heat maps of proportional parameter frequency. x axis indicates the parameter number (see Supplemental Materials and Methods for parameters and their corresponding number), y axis indicates the range of values using the base 10 scale. Since these parameters are for the non-dimensionalized model and represent groupings of biochemical rate constants, the parameters may range over many orders of magnitude despite potential constraints on the biochemical rate constants. (A) Distribution of parameter frequency using a modified Metropolis-Hastings random walk. Values range from 10^{-7} to $10^{8.5}$. Parameter 41, κ_{39} , LIN-39-mediated LAG-2 synthesis half max value, appears to be more constrained than other values although it still ranges over 5 orders of magnitude. (B) Distribution of parameter frequency using a strictly random sampling algorithm. Values range from 10^{-2} to 10^2 but are plotted on the same scale as the random walk values for ease of comparison. Parameters generated by both methods tend to cluster around the same values, but the values generated by the random walk are not constrained to fall within a specified range. (C) Parameter 41 appears more constrained than the other parameters for both methods. However, it has a similar range and frequency regardless of the generating algorithm. Red represents values from the random sampling method and black represents values from the random walk method. Frequencies are normalized with respect to the total number of parameter sets generated by the two sampling methods.

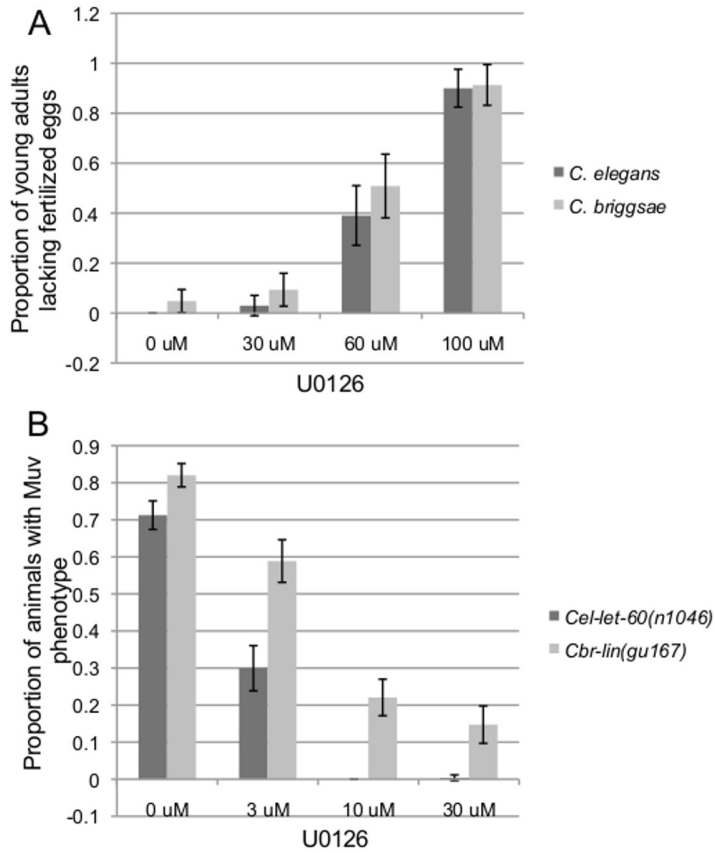


Figure S2: **The MEK inhibitor U0126 is effective in *C. elegans* and *C. briggsae*.** (A) Treatment of wild-type *C. elegans* and *C. briggsae* animals with U0126 has a similar dose-response effect on animal fertility. (B) The Muv (extra vulval cell division) phenotype of *C. elegans* and *C. briggsae* mutants can be blocked to a similar extent by treatment with U0126.

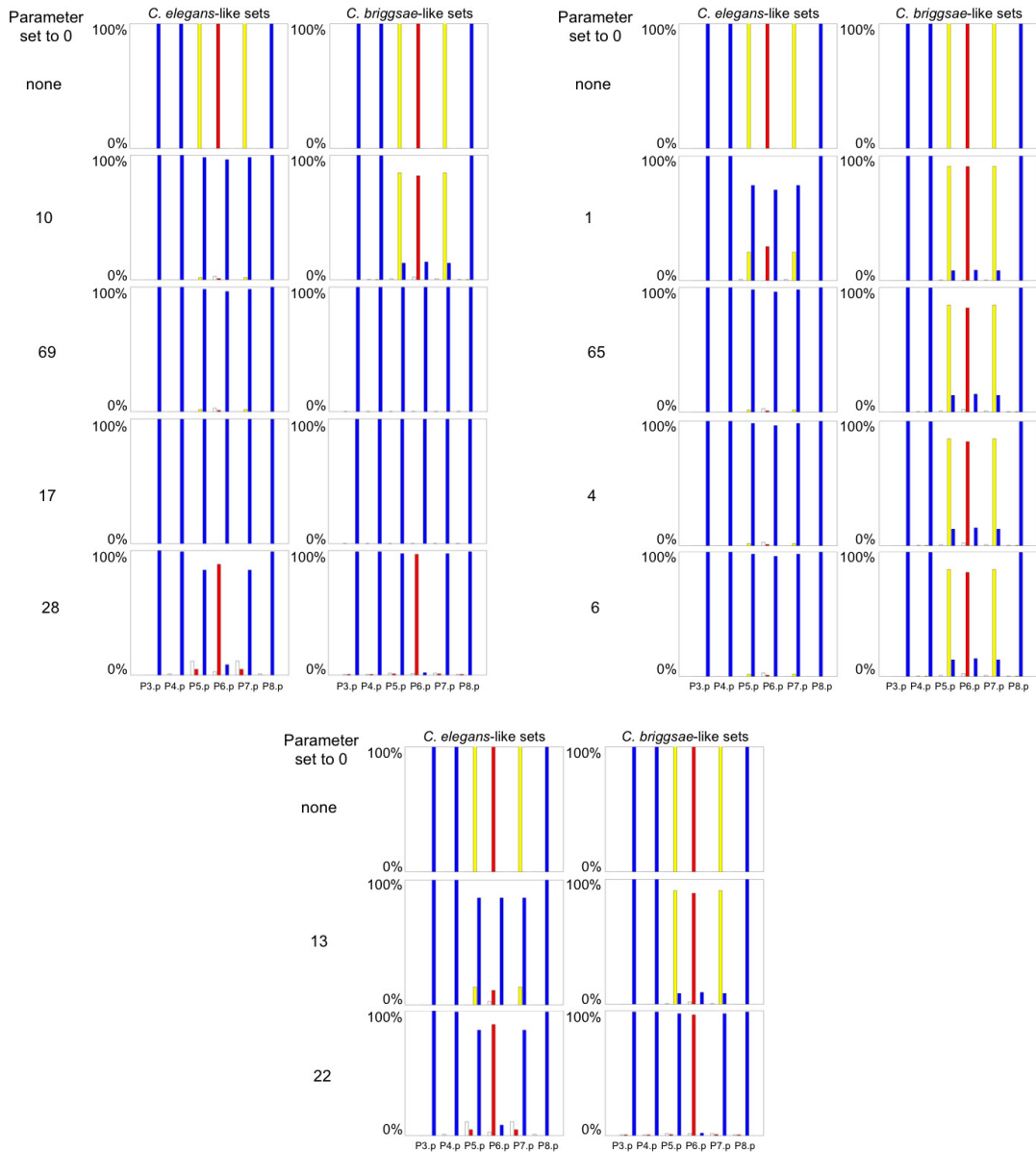


Figure S3: **The responses of *C. elegans* and *C. briggsae*-like parameter subsets in the model differ for EGF pathway but not other pathways when specific parameters are set to 0.** Bar graphs represent proportion of models that yield primary (red), secondary (yellow), tertiary (blue), or abnormal (white) behavior for the given cell (P3.p-P8.p) under conditions when specific parameters are set to 0. Results for parameters 10 (MPK-1 phosphorylation rate), 69 (Steepness of WNT gradient and WNT signal strength at P5.p, P7.p), 17 (LIN-39 combined synthesis/decay rate), 28 (LIN-12 synthesis rate), 1 (k_{23min}^- , Min LET-23 synthesis rate); 65 (*LN3b*, Steepness of LIN-3 gradient and LIN-3 signal strength at P5.p, P7.p); 4 (k_{60}^+ , LET-60 activation rate); 6 (k_{45}^+ , LIN-45 phosphorylation rate); 13 (k_{11}^+ , LIN-1 phosphorylation rate); 22 (k_{ni}^- , NICD combined synthesis/decay rate).

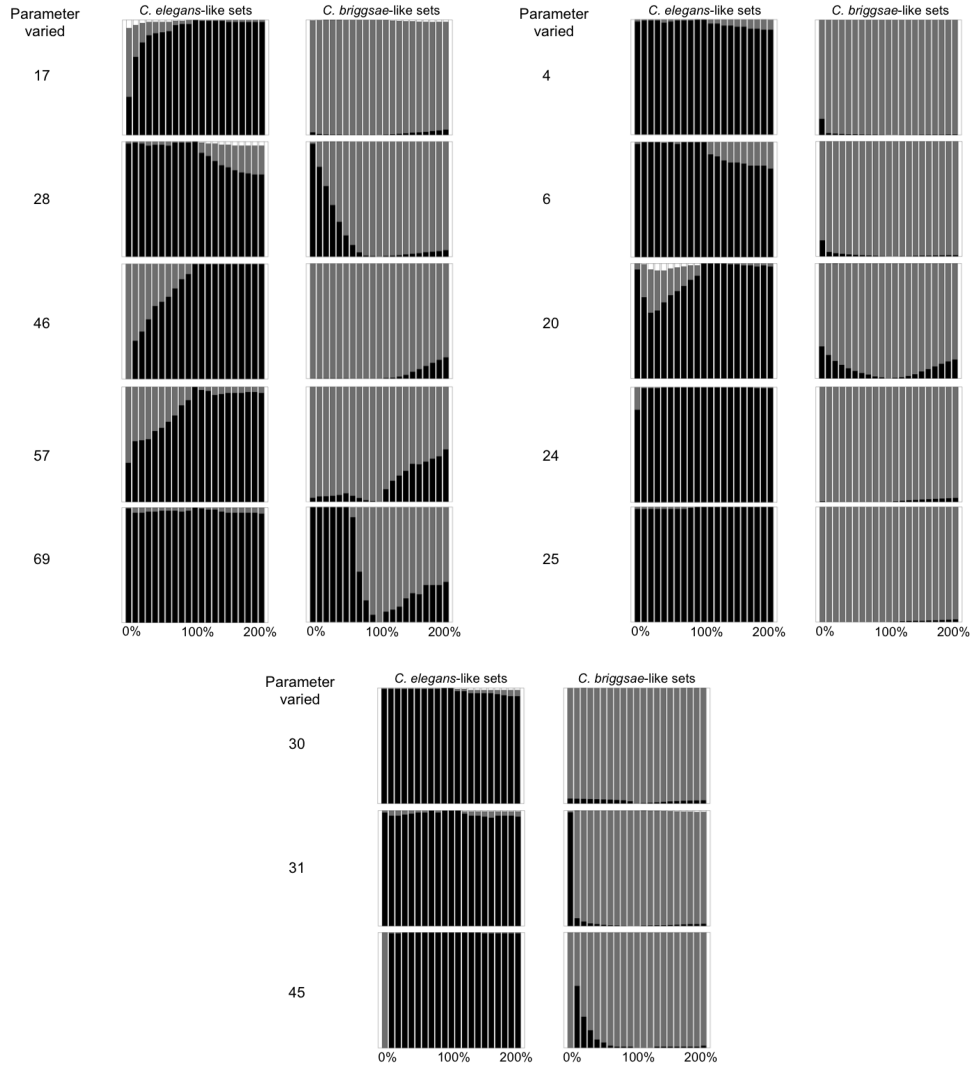


Figure S4: **Model behavior in response to parameter variation.** Stacked bar graphs summarizing the response of all members of the *C. elegans* and *C. briggsae*-like parameter subsets to variation of the parameters identified in Table 2 (Main text) that exhibit significant differences in value between the *C. elegans* and *C. briggsae* sets. In all of the simulations, the parameter listed in the left column was varied from 0% to 200% (in 10% increments), with the additionally challenge of altered levels of k_{mp}^+ (inhibition of MEK-2 activity to 30% of normal). Black indicates a *C. elegans*-like response of the model when the given parameter is altered. Gray indicates a *C. briggsae*-like response. Five parameters that exhibited a “switching” response in one or the other species include 17 (k_{39}^- , LIN-39 combined synthesis/decay rate); 28 (β_{l12} , LIN-12 synthesis rate); 46 (κ_{nic} , NICD-mediated LIP-1 synthesis half max value); 57 (n_{39} , LIN-39-mediated LAG-2 synthesis Hill exponent); 69 (*WNTb*, Steepness of WNT gradient and WNT signal strength at P5.p, P7.p.). Other parameters tested include 4 (k_{60}^+ , LET-60 activation rate); 6 (k_{45}^+ , LIN-45 phosphorylation rate); 20 (k_{n12min}^- , Min SUR-2-mediated LIN-12 decay); 24 (k_{ak}^- , ARK-1 combined synthesis/decay rate); 25 (β_{23} , LET-23 combined phosphorylation/dephosphorylation rate); 30 (β_{l123} , LAG-2/LIN-12 complex dissociation rate); 31 (β_{212} , LAG-2/LIN-12 complex combined formation/dissociation rate); 45 (κ_{sr22} , SUR-2-mediated LIN-12 synthesis half max value).

References

- [1] P. W. Sternberg, A. Golden, and M. Han, "Role of a raf proto-oncogene during *Caenorhabditis elegans* vulval development.," *Philosophical transactions of the Royal Society of London. Series B, Biological sciences*, vol. 340, pp. 259–65, jun 1993.
- [2] P. W. Sternberg, G. Lesa, J. Lee, W. S. Katz, C. Yoon, T. R. Clandinin, L. S. Huang, H. M. Chamberlin, and G. Jongeward, "LET-23-mediated signal transduction during *Caenorhabditis elegans* development," *Molecular reproduction and development*, vol. 42, pp. 523–528, dec 1995.
- [3] a. Hajnal, C. W. Whitfield, and S. K. Kim, "Inhibition of *Caenorhabditis elegans* vulval induction by gap-1 and by let-23 receptor tyrosinekinase," *Genes & Development*, vol. 11, pp. 2715–2728, oct 1997.
- [4] R. J. Hill and P. W. Sternberg, "The gene lin-3 encodes an inductive signal for vulval development," *Nature*, vol. 358, pp. 470–6, aug 1992.
- [5] R. V. Aroian, M. Koga, J. E. Mendel, Y. Ohshima, and P. W. Sternberg, "The let-23 gene necessary for *Caenorhabditis elegans* vulval induction encodes a tyrosine kinase of the EGF receptor subfamily," *Nature*, vol. 348, no. 6303, pp. 693–699, 1990.
- [6] J. S. Simske and S. K. Kim, "Sequential signalling during *Caenorhabditis elegans* vulval induction.," *Nature*, vol. 375, pp. 142–6, may 1995.
- [7] M. Han, R. V. Aroian, and P. W. Sternberg, "The let-60 locus controls the switch between vulval and nonvulval cell fates in *Caenorhabditis elegans*," *Genetics*, vol. 3, pp. 899–913, dec 1990.
- [8] P. S. Kayne and P. W. Sternberg, "Ras pathways in *Caenorhabditis elegans*," *Current opinion in genetics & development*, vol. 5, pp. 38–43, mar 1995.
- [9] M. Han, A. Golden, Y. Han, and P. Sternberg, "C. elegans lin-45 raf gene participates in let-60 ras-stimulated vulval differentiation," *Nature*, vol. 363, pp. 133–140, 1993.
- [10] K. Kornfeld, K. L. Guan, and H. R. Horvitz, "The *Caenorhabditis elegans* gene mek-2 is required for vulval induction and encodes a protein similar to the protein kinase MEK.," *Genes & development*, vol. 9, pp. 756–68, mar 1995.
- [11] Y. Wu, M. Han, and K. L. Guan, "MEK-2, a *Caenorhabditis elegans* MAP kinase kinase, functions in Ras-mediated vulval induction and other developmental events.," *Genes & Development*, vol. 9, pp. 742–755, mar 1995.
- [12] D. Jacobs, G. J. Beitel, S. G. Clark, H. R. Horvitz, and K. Kornfeld, "Gain-of-function mutations in the *Caenorhabditis elegans* lin-1 ETS gene identify a C-terminal regulatory domain phosphorylated by ERK MAP kinase.," *Genetics*, vol. 149, pp. 1809–22, aug 1998.
- [13] P. B. Tan, M. R. Lackner, and S. K. Kim, "MAP Kinase Signaling Specificity Mediated by the LIN-1 Ets/LIN-31 WH Transcription Factor Complex during *C. elegans* Vulval Induction," *Cell*, vol. 93, pp. 569–580, may 1998.
- [14] D. Jacobs, D. Glossip, and H. Xing, "Multiple docking sites on substrate proteins form a modular system that mediates recognition by ERK MAP kinase," *Genes & ...*, pp. 163–175, 1999.

- [15] T. Tiensuu, M. K. Larsen, E. Vernersson, and S. Tuck, “lin-1 has both positive and negative functions in specifying multiple cell fates induced by Ras/MAP kinase signaling in *C. elegans*,” *Developmental biology*, vol. 286, pp. 338–51, oct 2005.
- [16] R. M. Howard and M. V. Sundaram, “*C. elegans* EOR-1/PLZF and EOR-2 positively regulate Ras and Wnt signaling and function redundantly with LIN-25 and the SUR-2 Mediator component,” *Genes & development*, vol. 16, pp. 1815–27, jul 2002.
- [17] N. Singh and M. Han, “sur-2, a novel gene, functions late in the let-60 ras-mediated signaling pathway during *Caenorhabditis elegans* vulval induction,” *Genes & development*, vol. 9, pp. 2251–2265, sep 1995.
- [18] D. D. Shaye and I. Greenwald, “LIN-12/Notch trafficking and regulation of DSL ligand activity during vulval induction in *Caenorhabditis elegans*,” *Development (Cambridge, England)*, vol. 132, pp. 5081–92, nov 2005.
- [19] J. a. Wagmaister, J. E. Gleason, and D. M. Eisenmann, “Transcriptional upregulation of the *C. elegans* Hox gene lin-39 during vulval cell fate specification,” *Mechanisms of development*, vol. 123, pp. 135–50, feb 2006.
- [20] J. N. Maloof and C. Kenyon, “The Hox gene lin-39 is required during *C. elegans* vulval induction to select the outcome of Ras signaling,” *Development (Cambridge, England)*, vol. 125, pp. 181–90, jan 1998.
- [21] J. E. Gleason, H. C. Korswagen, and D. M. Eisenmann, “Activation of Wnt signaling bypasses the requirement for RTK/Ras signaling during *C. elegans* vulval induction,” *Genes & development*, vol. 16, pp. 1281–90, may 2002.
- [22] J.-B. Pénigault and M.-A. Félix, “High sensitivity of *C. elegans* vulval precursor cells to the dose of posterior Wnts,” *Developmental biology*, vol. 357, pp. 428–38, sep 2011.
- [23] N. Chen and I. Greenwald, “The lateral signal for LIN-12/Notch in *C. elegans* vulval development comprises redundant secreted and transmembrane DSL proteins,” *Developmental cell*, vol. 6, pp. 183–92, feb 2004.
- [24] M. Baron, “An overview of the Notch signalling pathway,” *Seminars in Cell & Developmental Biology*, vol. 14, pp. 113–119, apr 2003.
- [25] T. Berset, E. F. Hoier, G. Battu, S. Canevascini, and a. Hajnal, “Notch inhibition of RAS signaling through MAP kinase phosphatase LIP-1 during *C. elegans* vulval development,” *Science (New York, N.Y.)*, vol. 291, pp. 1055–8, feb 2001.
- [26] A. S. Yoo, C. Bais, and I. Greenwald, “Crosstalk between the EGFR and LIN-12/Notch pathways in *C. elegans* vulval development,” *Science (New York, N.Y.)*, vol. 303, pp. 663–6, jan 2004.
- [27] X. Zhang and I. Greenwald, “Spatial regulation of lag-2 transcription during vulval precursor cell fate patterning in *Caenorhabditis elegans*,” *Genetics*, vol. 188, pp. 847–58, aug 2011.
- [28] D. Shaye and I. Greenwald, “Endocytosis-mediated downregulation of LIN-12/Notch upon Ras activation in *Caenorhabditis elegans*,” *Nature*, vol. 420, no. December, 2002.

- [29] K. Takács-Vellai, T. Vellai, E. B. Chen, Y. Zhang, F. Guerry, M. J. Stern, and F. Müller, “Transcriptional control of Notch signaling by a HOX and a PBX/EXD protein during vulval development in *C. elegans*,” *Developmental biology*, vol. 302, pp. 661–9, feb 2007.
- [30] N. a. Hopper, J. Lee, and P. W. Sternberg, “ARK-1 inhibits EGFR signaling in *C. elegans*,” *Molecular cell*, vol. 6, pp. 65–75, jul 2000.
- [31] N. Moghal, “The epidermal growth factor system in *caenorhabditis elegans*,” *Experimental Cell Research*, vol. 284, pp. 150–159, mar 2003.
- [32] E. Hoyos, K. Kim, J. Milloz, M. Barkoulas, J.-B. Pénigault, E. Munro, and M.-A. Félix, “Quantitative variation in autocrine signaling and pathway crosstalk in the *Caenorhabditis* vulval network,” *Current biology : CB*, vol. 21, pp. 527–38, apr 2011.
- [33] S. Agrawal, C. Archer, and D. V. Schaffer, “Computational models of the Notch network elucidate mechanisms of context-dependent signaling,” *PLoS computational biology*, vol. 5, p. e1000390, may 2009.
- [34] N. Kravtsova, H. M. Chamberlin, and A. T. Dawes, “Modified Metropolis-Hastings algorithm for efficiently searching parameter space,” no. Mcmc, pp. 1–6.
- [35] W. P. Gardiner, *Statistical Analysis Methods for Chemists: A Software-based Approach*. Royal Society of Chemistry, 1997.